

# Processing and Decoding Rydberg Decay Error with MBQC

Cheng-Cheng Yu,<sup>1,2,3</sup> Zi-Han Chen,<sup>1,2,3</sup> Yu-Hao Deng,<sup>1,2,3</sup>  
Ming-Cheng Chen,<sup>1,2,3</sup> Chao-Yang Lu,<sup>1,2,3</sup> and Jian-Wei Pan<sup>1,2,3</sup>

<sup>1</sup>*Hefei National Research Center for Physical Sciences at the Microscale and School of Physical Sciences,  
University of Science and Technology of China, Hefei 230026, China*

<sup>2</sup>*Shanghai Research Center for Quantum Science and CAS Center  
for Excellence in Quantum Information and Quantum Physics,*

*University of Science and Technology of China, Shanghai 201315, China*

<sup>3</sup>*Hefei National Laboratory, University of Science and Technology of China, Hefei 230088, China*

Achieving fault-tolerant quantum computing with neutral atom necessitates careful consideration of the errors inherent to this system. One typical error is the leakage from Rydberg states during the implementation of multi-qubit gates, which may propagate to multiple correlated errors and deteriorate the performance of error correction. To address this, researchers have proposed an erasure conversion protocol that employs fast leakage detection and continuous atomic replacement to convert leakage errors into benign erasure errors. While this method achieves a high threshold and a favorable error distance  $d_e = d$ , its applicability is restricted to certain atom species. In this work, we present a novel approach to manage Rydberg decay errors in measurement-based quantum computation (MBQC). From a hardware perspective, we utilize practical experimental techniques along with an adaptation of the Pauli twirling approximation (PTA) to mitigate the impacts of leakage error, which propagates similarly to Pauli error without degrading the error distance. From a decoding perspective, we leverage the inherent structure of topological cluster states and final leakage detection information to locate propagated errors from Rydberg decay error. This approach eliminates the need for mid-circuit leakage detection, while maintaining an error distance  $d_e = d$  and achieving a high threshold of 3.617(3)% per CZ gate for pure Rydberg decay. In the presence of additional Pauli errors, we demonstrate the performance of our protocol in logical error rate within a reasonable range of physical errors and draw a comparison with erasure conversion. The results show a comparable performance within a modest  $R_e$ , which reveals possible application of our method in near-term platform.

## I. INTRODUCTION

Neutral atom array has emerged as a promising platform for quantum computing [1–4]. High-fidelity quantum operations have been demonstrated for different atom species [5–8] and IQP sampling in logical qubits has been demonstrated for <sup>87</sup>Rb [9]. For neutral atoms, leakage error from Rydberg state (we refer this as Rydberg decay error), including blackbody radiation (BBR) and radiative decay (RD), is a dominant error source [10, 11]. Leakage error is particularly harmful because a single leakage error may induce two-qubit error chain through multi-qubit gate, which leads to a degraded error distance  $\lfloor \frac{d+3}{4} \rfloor$  compared to pauli error [12–15]. Researchers have shown that, with mid-circuit leakage detection, such error can be converted to erasure error, which has an error distance  $d$  [6, 7, 16–18]. However, mid-circuit leakage detection is limited to certain atom species. For <sup>171</sup>Yb atoms, BBR and RD can be respectively detected by fast ionization and cyclic transition [7, 16, 19]. Some preliminary demonstrations have shown decay errors to ground state in <sup>171</sup>Yb and <sup>88</sup>Sr are converted to erasure error [6, 7]. But for alkali atoms, detection of BBR needs measurement of ancilla qubit, which leads to heavy time overhead if mid-circuit leakage detected is needed [10, 11].

An equivalent model for quantum computation is MBQC, where large-scale entangled state is prepared in advance and measured sequentially to implement quan-

tum operation and process information [20–22]. Fault-tolerance of MBQC can be achieved by 3d RHG cluster state [23–26] that can be mapped to 2d surface code propagating in time [27–29]. MBQC is considered as a promising route for flying photon [22] and we point out that it also fits for neutral atom because outstanding scalability and connectivity in neutral atom platform provides potential convenience for entangled state generation. Besides, MBQC also has convenience to deal with the leakage (or qubit loss) [30]. In quantum circuit model, only a subset of qubit is measured when implementing syndrome measurement. Therefore if leakage happens on unmeasured qubit, it is undetected unless we introduce additional leakage detection [13, 30]. But in MBQC, every qubit is measured finally so the location of leakage can be detected to convert the error to less harmful erasure error, even through the error spread needs additional consideration.

In this article, we propose a novel protocol to deal with Rydberg decay error in RHG cluster state. From hardware perspective, we utilize practical experimental technique to minimize the harm of Rydberg decay. This is inspired by the property that a lost atom acts as  $|0\rangle$  during Rydberg interaction [16]. The processed Rydberg decay has similar error propagation to pauli error and thus does not degrade the distance. From decoding perspective, we utilize the inherent structure in RHG cluster state to locate the propagated error, with a specified three-outcome measurement to distinguish leaked

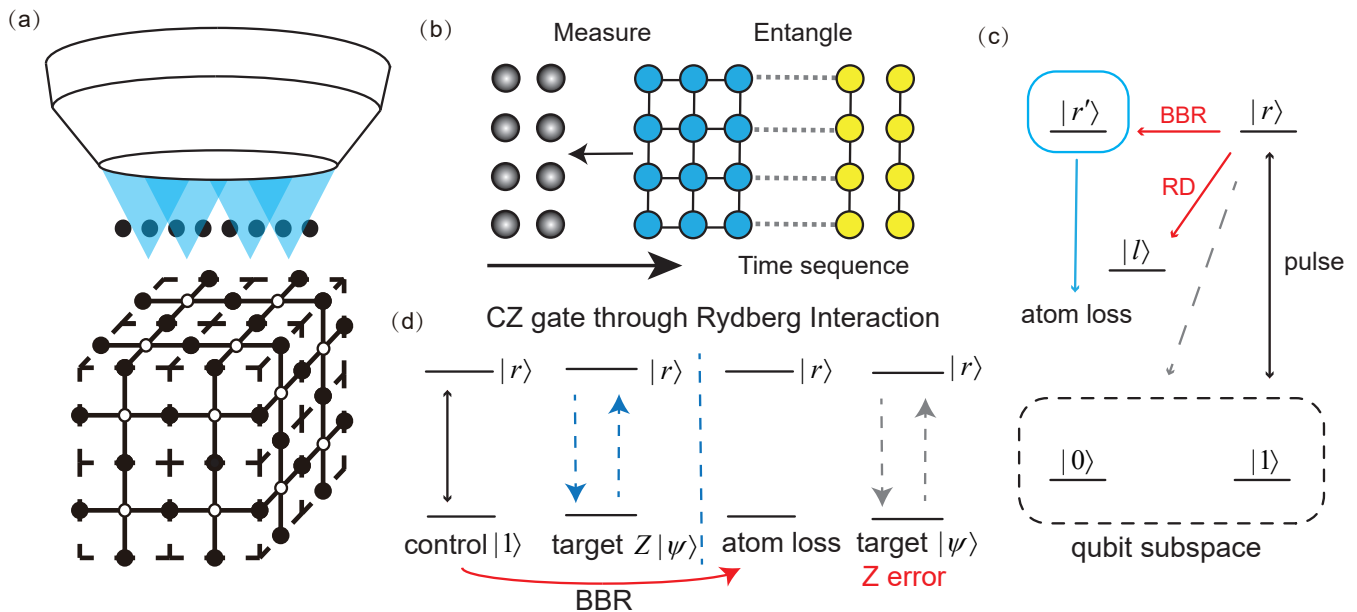


FIG. 1: (a) A schematic diagram for implementation of MBQC with neutral atoms. (b) In removable atoms array, we divide 3D RHG cluster state into 2D resource cluster state. Then we entangle the resource state with the 3D cluster state and measured the first layer in sequence. (c) Encoding for a neutral atom. Two low-lying states are used to encode physical qubit and only  $|1\rangle$  can be pumped onto Rydberg state  $|r\rangle$ . The leakage from Rydberg state  $|r\rangle$  has two branches, one leaks onto other Rydberg state  $|r'\rangle$  through BBR and another leaks to lower state through RD, including intermediate state scattering. Anti-trapping potential is needed to eject the atoms in Rydberg state after each CZ gate. This converts BBR error  $|r'\rangle$  to atom loss, preventing correlated pauli error from the decay of  $|r'\rangle$ . (d) When the atom is lost or jumps to a level that does not couple with the Rydberg state, it acts as if in state  $|0\rangle$  because it does not provide any Rydberg interaction. Compared to its initial state  $|1\rangle$ , this leakage propagates a Z error to the atom that has interacted with the leaked qubit. This describes the forward propagation of  $K_1$  or  $K_{1L}$ .

state and state in qubit subspace [11, 13, 29]. We develop a *matching-based* algorithm to decode the errors, by re-weighting the edges in decoding graph representing detector error model [31, 32]. The whole protocol is realized with no need for mid-circuit leakage detection. For pure Rydberg decay error, we demonstrate a high threshold 3.617% for each CZ gate and error distance  $d_e = d$ , which has significant improvement over previous work [30]. By considering the leakage together with two-qubit depolarization error in CZ gates, the threshold and error distance degrades because of a mixture with pauli error [16, 18]. We compare our method with erasure conversion and show that our method achieves a comparable logical error performance within a modest  $R_e$ , even without mid-circuit leakage detection [18]. Our work has proposed an alternative way for neutral atom qubits to achieve high performance in error correction and suggests the potential of MBQC for Rydberg atoms.

We first explain how we deal with Rydberg decay error and how to model them in circuit in Sec II and then explain the property of error distance in Sec III. In Sec IV, we develop the decoding protocol to locate the propagated error by Rydberg decay. In Sec V, we provide some numerical results for *pure Rydberg decay* condition and *general error* condition and discuss the performance

of our protocol. We conclude and give some discussions in Sec VI.

## II. FORMULATION OF RYDBERG DECAY ERROR MODEL

In this section, we formulate the model for Rydberg decay to connect how to manage Rydberg decay from a hardware perspective and the role of Rydberg decay in quantum error correction. For a frequently-used encoding shown in Fig 1(c), the channel of Rydberg decay is described in the operator-sum form, with two kraus operators  $\xi(\rho) = \sum_{i=0,1} K_i \rho K_i^\dagger$  [10, 18].

$$\begin{cases} K_0 = |0\rangle\langle 0| + \sqrt{1-p_e}|1\rangle\langle 1| + |L\rangle\langle L| \\ K_1 = \sqrt{p_e}|L\rangle\langle 1| \end{cases} \quad (1)$$

We refer to  $K_0$  as no-jump evolution and  $K_1$  as jump operator in this article. We don't consider the jump operators between qubit subspace that are modeled as pauli error with Pauli twirling approximation (PTA), because pauli errors are compatible with traditional error correction schemes. We discuss how to deal with the leaked state  $|L\rangle$  from a hardware perspective in Sec II A. We

then develop an adapted Pauli twirling in the presence of leaked state in Sec II B. We conclude on our error model in Sec II C. We only consider single qubit Rydberg decay channel because correlated Z error introduced by two-qubit Rydberg decay channel is to second order and does not influence our decoding [18].

### A. Rydberg decay from hardware perspective

In previous works, Rydberg decay always comes along with a re-initialization process, including replacing the leaked atoms with new atoms in state  $|1\rangle$  [18] and waiting until the Rydberg population turns back to qubit subspace [7, 15]. These two methods both lead to large time-overhead, because the first method needs movement of atoms from reservoir and the second leads to an idling time proportional to Rydberg state lifetime.

We take a different approach that directly deals with the leaked state  $|L\rangle$ . As is discussed in [10], leaked state  $|L\rangle$  includes Rydberg state  $|r\rangle$  or other hyperfine state  $|f\rangle$  (or ground state  $|g\rangle$ ) for alkaline-earth atom [16]. Population in Rydberg state can be converted to atom loss by applying anti-trapping light to eject the atoms. Faster alternative methods including laser induced or field induced ionization [10, 11] and a fast microwave-enhanced process to convert  $|r\rangle$  to atom loss is demonstrated in [33]. One important feature is that the lost atoms are not involved in Rydberg interaction anymore so it acts as  $|0\rangle$ . This suggests that the error channel of Rydberg decay is similar to that of amplitude damping [34], but the leaked state (or atom loss) can be distinguished from qubit subspace with three-outcome measurement [11, 13]. Above discussion for BBR is also applicable for RD as long as the leaked state from RD does not couple to single or two-qubit drive laser. This requirement is naturally satisfied by  $^{171}\text{Yb}$  because the majority of RD is to ground state  $|g\rangle$ , which is energetically separated from the qubit subspace [16]. For alkali atoms that use hyperfine states to encode a qubit, magnetic field is applied to separate qubit subspace and leaked state [11] or leaked state can be shelved to an isolated state via microwave pumping [35].

### B. Pauli twirling approximation and gate operation in the presence of leaked state

Given the process above, we expand the qubit subspace with leakage subspace with direct sum  $P'_i = P_i \oplus |L\rangle \langle L|$  ( $P_i = I, X, Y, Z$ ) [36]. For CZ gates we considered,  $CZ = I' \otimes I' - 2|11\rangle \langle 11|$  because the leaked state is not involved in CZ gates. Then we consider Rydberg decay channel Eq. 1. Even though the jump operator  $K_1$  propagates a Z error through CZ gates (See Appendix A), no-jump evolution  $K_0$  leads to off-diagonal terms in the process matrix [18, 34]. Such kind of coherent error may threaten to the performance of error correction [37]

despite TN decoder has revealed the consistency in performance of QEC between amplitude damping and its PTA counterpart [38]. Therefore, we need to apply PTA by inserting random pauli before and after each layer of CZ gates [39].

But the picture of PTA changes when the leaked state is in presence. The difference lies in the fact that, the pauli gate after the jump operator does not act anymore. We conclude the picture here and leave concrete derivation in Appendix A: The no-jump evolution leads to Z error to second order as mentioned in previous article [18, 34] but the jump operator  $K_1$  representing *biased erasure channel* is converted to two jump operators  $K_{0L}$  and  $K_{1L}$  representing *erasure channel* [40, 41]. Therefore, our protocol has naturally tolerated atom loss in neutral atoms platform [10, 42].

$$\begin{cases} K_{0L} = \sqrt{p_e/2} |L\rangle \langle 0| \\ K_{1L} = \sqrt{p_e/2} |L\rangle \langle 1| \end{cases} \quad (2)$$

In this adaptation to usual PTA, we can not consider the error as random pauli error. A possible method is to forward-propagating, namely an error  $E$  before some unitary  $U$  equals to  $UEU^\dagger$  after the unitary [43]. We prove  $K_{0L}$  commutes with CZ gates used in generating RHG cluster state and  $K_{1L}$  propagates a Z error through CZ gate if the interacted qubit is not leaked (See Appendix A). We name this kind of error propagation as *deterministic error propagation* because the leakage error (one jump operator  $K_{1L}$ ) deterministically propagates a pauli error to each qubit that interacts with it. The picture of above discussion is concluded in Fig.2.

### C. Model of Rydberg decay in QEC

We model Rydberg decay from two aspects: the error during each CZ gate and the error propagation. For each CZ gate, if the two qubit are both in qubit subspace, we assume that one of the two qubit leaks and totally dephase the other one with probability  $p_e$  (tailored Z channel [36, 44]). Namely, we draw an operator from  $\frac{p_e}{4}\{L \otimes I, L \otimes Z, I \otimes L, Z \otimes L\}$  ( $L$  refers to  $K_{0L}$  or  $K_{1L}$ ). This error model can be considered as a adaptation from the model in [18]. Here we ignored  $L \otimes L$  for the reason that we find  $L \otimes L$  is less harmful than one leakage instance when we decode topological cluster state, as explained in Appendix C. We then utilize the operator-sum form to model the error propagation. To simulate the error propagation, we sample from two kraus operator ( $K_{0L}$  and  $K_{1L}$ ) with equal propability if a leakage ( $L$ ) happens. This is to sample the pauli matrix before the jump operator ( $X, Y$  or  $I, Z$ ). If the sampled jump operator is  $K_{0L}$ , it will not propagate error through CZ gates. For  $K_{1L}$ , it propagates Z error to proximal qubits through residual CZ gates. The error propagation is similar to an X error. When an unleased qubit interacts with another, the unleased qubit encounters leakage errors as

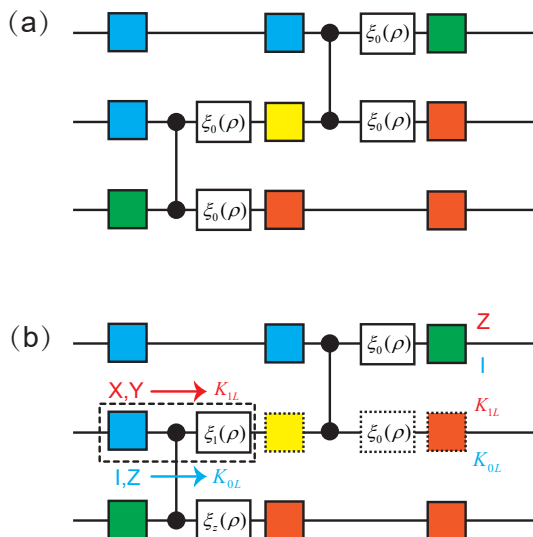


FIG. 2: PTA in the presence of leaked state. Different colored squares represent different pauli operators, which are determined by randomized compiling [39]. White rectangles represent different channels.  $\xi_0(\rho)$ ,  $\xi_1(\rho)$  are no-jump evolution and jump evolution defined by  $K_0$  and  $K_1$ .  $\xi_Z(\rho)$  is tailored Z error, representing a leakage during gate operation totally dephases another qubit. (a) For no-jump evolution, PTA cancels non-diagonal term in process matrix. (b) If the second qubit encounters a jump operator, subsequent pauli operator and no-jump evolution do not act non-trivially (dashed line). Effective jump operator is determined by the pauli operator before. The error propagation is considered by forward-propagating.

usual but does not encounter totally dephasing error because its interacting qubit is not leaked during the gate sequence. For propagated pauli error from Rydberg decay, adjacent qubits only encounter deterministic error propagation from their interacting qubits, depending on the kraus operator ( $K_{0L}$  and  $K_{1L}$ ) sampled before [45].

### III. PROPERTY OF ERROR DISTANCE OF RYDBERG DECAY

In this section, we give some discussions about *error distance*  $d_e$  of Rydberg decay (Sometimes error distance is referred to as error dimension [46, 47]). Error distance is the minimum number of physical qubit error needed to generate a logical error. It is related to sub-threshold scaling of logical error rate. When physical error rate is small enough, logical error rate is suppressed exponentially with error distance  $d_e$ , namely  $p_L \sim (p/p_{th})^{d_e}$  [16, 48]. Therefore high error distance is desired to achieve good performance in QEC.

Error distance is influenced by two factors. One is whether the error is located and another is whether one error induce two qubit error chain along the logical op-

erator. For the first factor, an error correction code with code distance  $d$  corrects  $d - 1$  located errors (erasure errors) but  $\lfloor \frac{d}{2} \rfloor$  pauli errors [16, 49]. ‘located’ means that we know which qubits (or gates for detector error model [32]) is suspicious to be faulty so a detected leakage error is a located erasure error. Error propagation is another question. Under some circumstances, single error in ancilla qubit leads to two qubit error chain in data qubits along the logical operator. In rotated surface code only tolerates  $\lfloor \frac{d}{4} \rfloor$  ancilla errors a *bad order* of stabilizer measurement circuit, instead of  $\lfloor \frac{d}{2} \rfloor$  [46, 50]. If a leakage error propagates to depolarization error, error correction code only tolerates  $\lfloor \frac{d}{4} \rfloor$  errors because no sequence exists to eliminate all error chains that degrade the distance [12–15, 30].

Previous work, erasure conversion, has shown an error distance  $d_e = d$  in different codes by mid-circuit leakage detection and atom replacement [16]. Leakage detection helps to locate the error and the introduced error by atom re-initialization are modeled by two-qubit pauli error. Therefore, erasure conversion generally leads to error distance  $d_e = d$ . The consideration is similar in our protocol. The error propagation in our protocol can also be considered by two-qubit pauli error because the jump operator deterministically propagates a pauli error. For example,  $L \otimes Z$  instance in CZ gate leads to the same error propagation with  $I \otimes Z$  and  $X \otimes Z$ . We emphasize that the mechanism that preserves the distance here is slightly different from that in surface code [36, 44]. Leakage error with tailored-pauli model preserves the distance in surface code but degrades the distance in RHG cluster state. Since the propagation of leakage is not harmful again, we are able to remove mid-circuit leakage detection and atom replacement and we use final measurement to approximately locate the error [42, 44, 51], as will be elaborated in Sec IV.

### IV. DECODING PROTOCOL FOR RYDBERG DECAY ERROR IN RHG CLUSTER STATE

In this section, we explain how we decode Rydberg decay errors in RHG cluster state. For clarity, we only consider Rydberg decay errors and perfect leakage detections now. RHG cluster state can be considered as a variant of surface code in MBQC form [27, 28]. The decoding protocol can be explained following Fig.3. To generate a RHG cluster state, we prepare all the qubits in state  $|+\rangle$  and then connect the qubits with CZ gates. Our simulation accounts for the noise in CZ gates used in state generation circuit Fig 3(b). In MBQC, each qubit is measured so a leakage error or atom loss can be naturally detected and converted to a more benign erasure error without mid-circuit detection. This specific measurement reports a leakage event if the measured qubit is lost or leaked. Otherwise it acts as a projective measurement [11, 13]. This measurement can be considered as a traditional projective measurement together with a fast

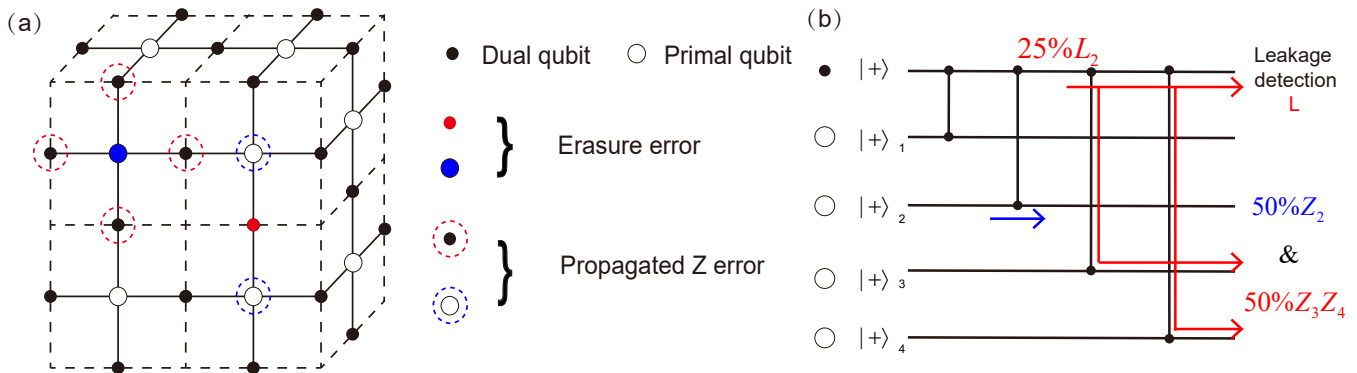


FIG. 3: Decoding protocol for Rydberg decay error (a)  $2 \times 2 \times 1$  lattice structure of RHG cluster state. In a cell of RHG cluster state, each dual qubit is connected to 4 primal qubits through CZ gate and the same for primal qubit. If a leakage is detected in dual qubit, we can calculate propagated Z error probability with the circuit in (b). For leakage in dual qubit, the same procedure is implemented by exchanging the position of primal qubit and dual qubit. (b) (Partial) circuit to generate RHG cluster state when we consider propagated Z errors in primal qubits. Each qubit is initialized in  $|+\rangle$  and is connected to neighboring qubits by CZ gate. If a leakage is detected finally in a dual qubit, it happens at four error sites with approximately equal probability 25% ( $L_i$  represents the dual qubit leaks at the  $i$ -th CZ gate). Each error site triggers some error mechanisms (edges in detector error model [32].) For example, if  $L_2$  happens in considered dual qubit, it dephases the second primal qubit ( $50\%Z_2$ ) and propagates to  $Z_3Z_4$  with 50% probability (depending on the jump operator,  $K_{0L}$  or  $K_{1L}$ ).

leakage detection [16] (or leakage detection units [10, 11]).

Our decoding is based on *Pymatching* (MWPM algorithm) [31] and *detector error model* [32]. The core idea of our decoding protocol is to use leakage detection information in dual (primal) lattice to approximately locate the propagated error in primal (dual) lattice. We refer to approximately locate error as *erasure-like error*. When qubits in the RHG cluster state are measured, the specific measurements above also tell us whether each qubit is leaked or not. Syndromes on the primal lattice and dual lattice are decoded separately in the same manner for error correction [52]. Taking primal lattice for decoding, we first record all leaked face qubits of primal lattice (we refer to them as primal qubits for convenience). These errors are directly located and converted to erasure errors and we assign the weights of the edges representing that qubit in decoding graph to 0, in MWPM algorithm [31, 53, 54]. Then, for each dual qubit, if it is detected to be leaked, it encounters a leakage  $L$  in one of the CZ gates with 25% probability for each (approximation to first order). We consider all possible error mechanisms and re-weight the edges representing these error mechanisms with average probabilities. For example, if a dual qubit leaks during the second CZ gate, it dephases the second primal qubit ( $50\%Z_2$ ) and at the same time propagates to  $50\%Z_3Z_4$ , triggering two error mechanisms. (For more details, see Appendix C).

## V. NUMERICAL RESULTS

In this section, we give some numerical results to demonstrate the performance of our protocol. We first

simulate a *pure Rydberg decay* error model where only Rydberg decay error is considered. We then simulate a more general error model by taking two-qubit depolarization into consideration. The consideration of depolarization error is included in Appendix D). The decoding graph is constructed with *stim* [32] and decoded with *pymatching* [31]. A discussion about gate sequence and propagated Z error chain is included in Appendix B.

### A. Pure Rydberg Decay

The results are shown in FIG.4. We demonstrate the threshold of leakage probability of each CZ gate and the error distance. To show the threshold, we sample  $10^5$  instances for  $d^3$  cubic lattices with periodic boundary condition for  $d = 3, 5, 7, 9, 11$ . The threshold gives 3.617(3)%, already significantly higher than the infidelity shown in recent experiments. To show the error distance, we sample  $2 * 10^7$  instances for  $d = 3$  and  $4 * 10^7$  for  $d = 4$  when physical error rate is well below threshold ( $p_e < 10^{-0.6}p_{th}$ ). The result shows that the approximate slope is  $d_e \approx d$ . Compared to previous result that  $d_e = \lfloor \frac{d+3}{4} \rfloor$ , our decoding protocol has a greatly improved error distance [30], which suggests a better suppression of logical error rate ( $p_L \sim (p/p_{th})^{d_e}$  when  $p = p_e \ll p_{th}$ ).

### B. General error

In this section, we show our decoding protocol is compatible with a more general error model by considering

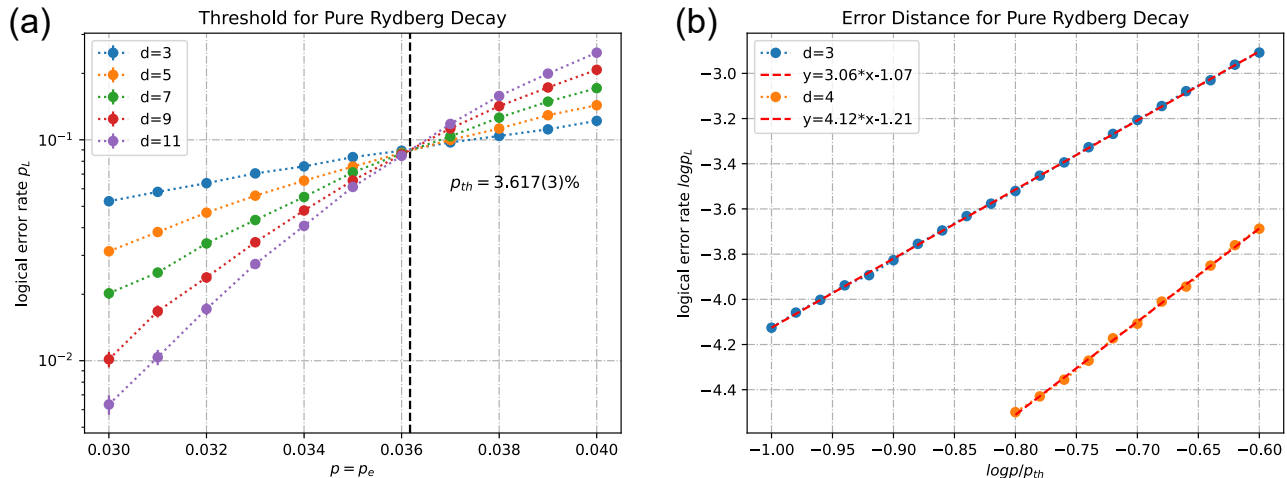


FIG. 4: Numerical results for pure Rydberg decay error model (a) Logical error rate for  $d = 3, 5, 7, 9, 11$ ,  $d^3$  cubic lattice of RHG cluster state. The threshold of leakage probability for each gate  $p_e = 3.617(3)\%$ , derived from cross point of  $d = 9$  and  $d = 11$ . (b) Error distances of our protocol. We do linear regression for  $\log p_L$  and  $\log p/p_{th}$  when  $p \ll p_{th}$  and the slope gives error distance. For our condition,  $d_e = 3.05(7)$  for  $d = 3$  and  $d_e = 4.12(1)$  for  $d = 4$ . The standard error of  $d_e$  is 0.009 and 0.041 respectively.

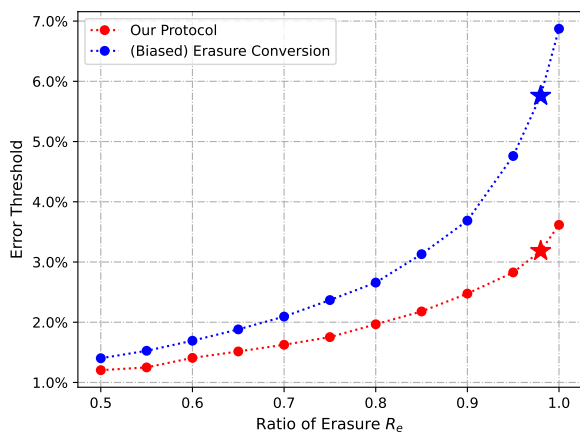


FIG. 5: The threshold changes when the ratio of erasure  $R_e$  changes, for both our protocol and erasure conversion. We consider a range of  $R_e$  from 0.5 to 1, taking the interval as 0.05. Besides,  $R_e = 0.98$ , a ratio of erasure from estimation of  $^{171}\text{Yb}$  atoms [16] is marked with stars by considering the branch of Rydberg decay. The results show that our protocol has higher threshold than traditional pauli error but lower threshold than biased erasure error.

two-qubit depolarization error and compare our results with previous erasure conversion (biased erasure, BE) [16, 18]. We need to emphasize that the performance of our protocol can never be better than erasure conversion because of additional error propagation induced by delayed leakage detection. It's a trade-off between exper-

imental requirements and performance of QEC. We refer to our method as leakage tracking (LT) for convenience, because we don't convert the leakage to erasure immediately but track the propagation of leakage error from final detection results.

We define the ratio of erasure  $R_e = p_e/p$  ( $p = p_p + p_e$  is the total error rate including pauli error rate  $p_p$  and leakage error rate  $p_e$ ). The threshold result is shown in Fig.5. For each threshold point we sample  $10^5$  for  $d = 9$  and  $d = 11$  and find the intersection point as threshold. When  $R_e$  is large ( $> 80\%$ ), the threshold of our protocol is exceeds 2%.

We also consider the logical error rate for  $d = 3, 5, 7$  when gate infidelity ranges from 0.1% to 1% and ratio of erasure  $R_e = 0.5, 0.7, 0.9$  to show sub-threshold performance [5–8], as shown in Fig.6 (For,  $d = 7$  several points are not plotted). Each point is sampled with at least  $10^8$  instances (at least 800 leakage instances each shot [51]). Pure pauli error is also plotted for comparison. Interestingly, Fig.6 reveals that leakage tracking method has an advantage in effective error distance over biased erasure conversion. We attribute the reason to the contribution of *erasure-like* error – when physical error rate is the same, LT method leads to additional *erasure-like* propagated error, which is suppressed faster than pauli error. Larger effective error distance narrows the gap between LT and EC when  $p$  decrease. We also prove that with small  $p$  and increasing  $d$ , ratio of logical error rate between two methods converges to a constant (independent of  $R_e$  and  $d$ ), which guarantee the performance of our protocol for future devices (See Appendix E for details).

The results is also important from practical perspec-

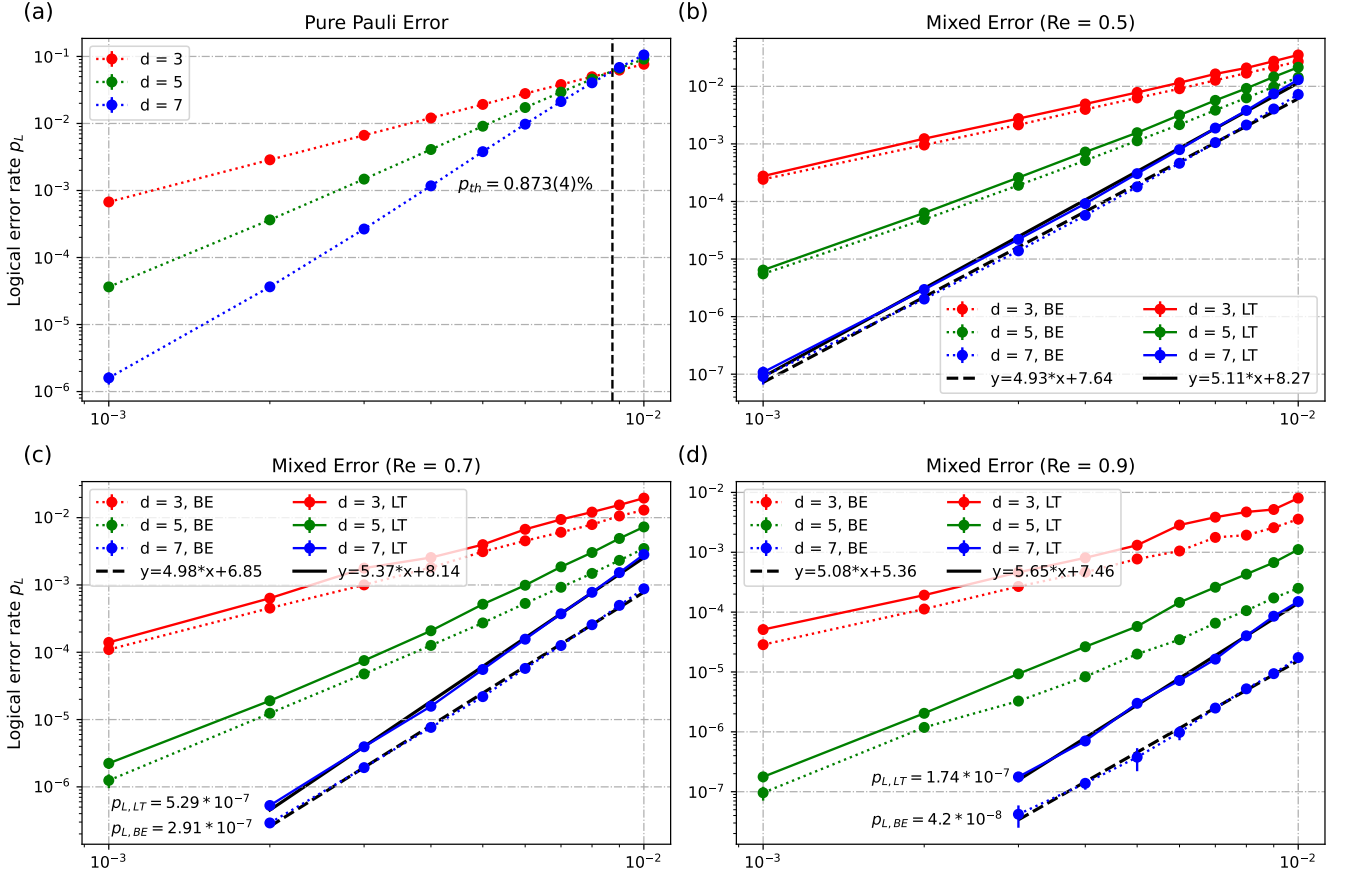


FIG. 6: Sub-threshold performance of our method with a mixture of pauli error and Rydberg decay error. Performance of pure pauli error and (biased) erasure conversion are also plotted for comparison. The slope is derived by linear regression of logical error rate and physical error rate in logscale, representing effective error distance in considered range. (a) Pure pauli error, the threshold gives 0.873(4)%. (b)  $R_e = 0.5$ . Error distance for BE and LT gives 4.92(8) and 5.10(5) respectively. (c)  $R_e = 0.7$ . Error distance for BE and LT gives 4.98(0) and 5.36(5) respectively. Logical error rate for  $d = 7, p = 0.2\%$  is marked out. (d)  $R_e = 0.9$ . Error distance for BE and LT gives 5.08(4) and 5.65(3) respectively. Logical error rate for  $d = 7, p = 0.3\%$  is marked out.

tive. There is always a balance between hardware-overhead and performance so people need to do a trade-off. Our results just show that, with a modest  $R_e$ , the difference in logical error rate is small. For example, for  $R_e = 0.7, p = 0.2\%$  and  $d = 7$ ,  $p_{L,LT} = 5.29 \times 10^{-7} < 2 * p_{L,EC}$ . But the hardware-overhead is always the same, no matter how large  $R_e$  is. This suggests that our leakage tracking method is a promising candidate, especially in the near-term when  $R_e$  is not large [7], limited by other noise sources in the current experimental system, in addition to Rydberg decay [5, 6, 8].

## VI. DISCUSSION AND OUTLOOK

Here we give some discussions about our protocol. We first propose to use available experimental technique to process Rydberg decay error and derive their propagating property from operator-sum form of the channel. We

find it propagates similar to a pauli error (we refer to it as *deterministic error propagation* in our article), which is beneficial in preserving error distance and improving the threshold [55]. Then, based on final leakage detection results, we infer the probabilities of propagated errors from Rydberg decay, thereby converting them to erasure-like errors. These allow us to achieve similar error distance as the erasure conversion protocol [16] for pure Rydberg decay errors. Comparing our protocol with previous work that directly deals with leakage error [30], we have greatly improved the threshold and we increase the error distance from  $\lfloor \frac{d+3}{4} \rfloor$  to  $d$ . To achieve this, the *deterministic error propagation* of Rydberg decay and innovative decoding protocol are both essential. For a general model that a leakage propagates to a depolarization error, our decoding protocol can only achieve  $d_e = \lfloor \frac{d+1}{2} \rfloor$ .

Then we compare our work with existing protocols to implement QEC in Rydberg atoms. An outstanding advantage of our protocol is that we deal with a wide range

of error source other than pauli error, including BBR, RD and atom loss [10]. Besides, our protocol can not only be used for  $^{171}\text{Yb}$ , but can be used for alkali atoms, with magnetic fields or shelving technique [35]. From hardware perspective, we have removed the use of mid-circuit leakage detection and atom replenishment utilized in erasure conversion [16, 18]. This is achieved by specific process for Rydberg decay to minimize the harm for leakage propagation. There are also some protocols that deal with BBR, RD and atom loss in neutral atoms respectively [10, 15, 29, 42]. Between these works, [42] has shown error distance  $d_e = d$  for atom loss with the help of leakage detection units (LDU) [11] and [29] has shown improved performance for different QEC protocols and for logical circuit, including MBQC (teleportation based SE). But their work is based on different error model with us so we also give some discussion in order to compare the performance (See Appendix F). Our works (together with previous work discussing imperfect erasure check

[44]) provide new insights to the properties of located error, which may inspire more hardware-efficient protocol related to located error [51].

For future work, one direction is to use BP algorithm to better locate the error [56] or to use correlated leakage  $L \otimes L$  to improve the performance of decoding. It is also important to implement MBQC experimentally in neutral atoms platform to demonstrate our protocol and the advantage in dealing with such leakage error.

*Note.- A related work [29] examines atom loss tolerance in logical circuits for various QEC protocols using an MLE decoder, including MBQC. They report a higher threshold than ours (4.61% vs 3.62%), but this difference primarily stems from the error model choice. Using our decoder with their error model achieves a 4.52% threshold. See Appendix F for details.*

- 
- [1] M. Saffman, T. G. Walker, and K. Mølmer. Quantum information with rydberg atoms. *Rev. Mod. Phys.*, 82:2313–2363, Aug 2010.
- [2] M Morgado and S Whitlock. Quantum simulation and computing with rydberg-interacting qubits. *AVS Quantum Science*, 3(2), 2021.
- [3] Adam M Kaufman and Kang-Kuen Ni. Quantum science with optical tweezer arrays of ultracold atoms and molecules. *Nature Physics*, 17(12):1324–1333, 2021.
- [4] Xiaoling Wu, Xinhui Liang, Yaoqi Tian, Fan Yang, Cheng Chen, Yong-Chun Liu, Meng Khoon Tey, and Li You. A concise review of rydberg atom based quantum computation and quantum simulation, 2021.
- [5] Simon J Evered, Dolev Bluvstein, Marcin Kalinowski, Sepehr Ebadi, Tom Manovitz, Hengyun Zhou, Sophie H Li, Alexandra A Geim, Tout T Wang, Nishad Maskara, et al. High-fidelity parallel entangling gates on a neutral-atom quantum computer. *Nature*, 622(7982):268–272, 2023.
- [6] Pascal Scholl, Adam L Shaw, Richard Bing-Shiun Tsai, Ran Finkelstein, Joonhee Choi, and Manuel Endres. Erasure conversion in a high-fidelity rydberg quantum simulator. *Nature*, 622(7982):273–278, 2023.
- [7] Shuo Ma, Genyue Liu, Pai Peng, Bichen Zhang, Sven Jandura, Jahan Claes, Alex P Burgers, Guido Pupillo, Shruti Puri, and Jeff D Thompson. High-fidelity gates and mid-circuit erasure conversion in an atomic qubit. *Nature*, 622(7982):279–284, 2023.
- [8] Michael Peper, Yiyi Li, Daniel Y. Knapp, Mila Bileska, Shuo Ma, Genyue Liu, Pai Peng, Bichen Zhang, Sebastian P. Horvath, Alex P. Burgers, and Jeff D. Thompson. Spectroscopy and modeling of  $^{171}\text{yb}$  rydberg states for high-fidelity two-qubit gates, 2024.
- [9] Dolev Bluvstein, Simon J Evered, Alexandra A Geim, Sophie H Li, Hengyun Zhou, Tom Manovitz, Sepehr Ebadi, Madelyn Cain, Marcin Kalinowski, Dominik Hangleiter, et al. Logical quantum processor based on reconfigurable atom arrays. *Nature*, 626(7997):58–65, 2024.
- [10] Iris Cong, Harry Levine, Alexander Keesling, Dolev Bluvstein, Sheng-Tao Wang, and Mikhail D Lukin. Hardware-efficient, fault-tolerant quantum computation with rydberg atoms. *Physical Review X*, 12(2):021049, 2022.
- [11] Matthew N. H. Chow, Vikas Buchemmavari, Sivaprasad Omanakuttan, Bethany J. Little, Saurabh Pandey, Ivan H. Deutsch, and Yuan-Yu Jau. Circuit-based leakage-to-erasure conversion in a neutral atom quantum processor, 2024.
- [12] Austin G. Fowler. Coping with qubit leakage in topological codes. *Phys. Rev. A*, 88:042308, Oct 2013.
- [13] Martin Suchara, Andrew W Cross, and Jay M Gambetta. Leakage suppression in the toric code. In *2015 IEEE International Symposium on Information Theory (ISIT)*, pages 1119–1123. IEEE, 2015.
- [14] Natalie C Brown, Andrew Cross, and Kenneth R Brown. Critical faults of leakage errors on the surface code. In *2020 IEEE International Conference on Quantum Computing and Engineering (QCE)*, pages 286–294. IEEE, 2020.
- [15] Sven Jandura and Guido Pupillo. Surface code stabilizer measurements for rydberg atoms, 2024.
- [16] Yue Wu, Shimon Kolkowitz, Shruti Puri, and Jeff D Thompson. Erasure conversion for fault-tolerant quantum computing in alkaline earth rydberg atom arrays. *Nature communications*, 13(1):4657, 2022.
- [17] Mingyu Kang, Wesley C Campbell, and Kenneth R Brown. Quantum error correction with metastable states of trapped ions using erasure conversion. *PRX Quantum*, 4(2):020358, 2023.
- [18] Kaavya Sahay, Junlan Jin, Jahan Claes, Jeff D Thompson, and Shruti Puri. High-threshold codes for neutral-atom qubits with biased erasure errors. *Physical Review X*, 13(4):041013, 2023.
- [19] Sivaprasad Omanakuttan, Vikas Buchemmavari, Michael J. Martin, and Ivan H Deutsch. Coherence preserving leakage detection and cooling in alkaline earth atoms, 2024.
- [20] Robert Raussendorf and Hans J. Briegel. A one-way

- quantum computer. *Phys. Rev. Lett.*, 86:5188–5191, May 2001.
- [21] Robert Raussendorf, Daniel E. Browne, and Hans J. Briegel. Measurement-based quantum computation on cluster states. *Phys. Rev. A*, 68:022312, Aug 2003.
- [22] Hans J Briegel, David E Browne, Wolfgang Dür, Robert Raussendorf, and Maarten Van den Nest. Measurement-based quantum computation. *Nature Physics*, 5(1):19–26, 2009.
- [23] Robert Raussendorf, Jim Harrington, and Kovid Goyal. A fault-tolerant one-way quantum computer. *Annals of physics*, 321(9):2242–2270, 2006.
- [24] Robert Raussendorf, Jim Harrington, and Kovid Goyal. Topological fault-tolerance in cluster state quantum computation. *New Journal of Physics*, 9(6):199, 2007.
- [25] Robert Raussendorf and Jim Harrington. Fault-tolerant quantum computation with high threshold in two dimensions. *Phys. Rev. Lett.*, 98:190504, May 2007.
- [26] Gabrielle Tournaire, Marvin Schwiering, Robert Raussendorf, and Sven Bachmann. A 3d lattice defect and efficient computations in topological mbqc, 2024.
- [27] A. Bolt, G. Duclos-Cianci, D. Poulin, and T. M. Stace. Foliated quantum error-correcting codes. *Phys. Rev. Lett.*, 117:070501, Aug 2016.
- [28] Benjamin J. Brown and Sam Roberts. Universal fault-tolerant measurement-based quantum computation. *Phys. Rev. Res.*, 2:033305, Aug 2020.
- [29] Gefen Baranes, Madelyn Cain, J. Pablo Bonilla Ataides, Dolev Bluvstein, Josiah Sinclair, Vladan Vuletic, Hengyun Zhou, and Mikhail D. Lukin. Leveraging atom loss errors in fault tolerant quantum algorithms, 2025.
- [30] Adam C. Whiteside and Austin G. Fowler. Upper bound for loss in practical topological-cluster-state quantum computing. *Phys. Rev. A*, 90:052316, Nov 2014.
- [31] Oscar Higgott and Craig Gidney. Sparse blossom: correcting a million errors per core second with minimum-weight matching. *arXiv preprint arXiv:2303.15933*, 2023.
- [32] Craig Gidney. Stim: a fast stabilizer circuit simulator. *Quantum*, 5:497, July 2021.
- [33] Sepehr Ebadi, Tout T. Wang, Harry Levine, Alexander Keesling, Giulia Semeghini, Ahmed Omran, Dolev Bluvstein, Rhine Samajdar, Hannes Pichler, Wen Wei Ho, Soonwon Choi, Subir Sachdev, Markus Greiner, Vladan Vuletić, and Mikhail D. Lukin. Quantum phases of matter on a 256-atom programmable quantum simulator. *Nature*, 595(7866):227–232, July 2021.
- [34] Akshaya Jayashankar, My Duy Hoang Long, Hui Khoon Ng, and Prabha Mandayam. Achieving fault tolerance against amplitude-damping noise. *Physical Review Research*, 4(2):023034, 2022.
- [35] T. M. Graham, L. Phuttitarn, R. Chinnarasu, Y. Song, C. Poole, K. Jooya, J. Scott, A. Scott, P. Eichler, and M. Saffman. Midcircuit measurements on a single-species neutral alkali atom quantum processor. *Phys. Rev. X*, 13:041051, Dec 2023.
- [36] Natalie C. Brown and Kenneth R. Brown. Leakage mitigation for quantum error correction using a mixed qubit scheme. *Phys. Rev. A*, 100:032325, Sep 2019.
- [37] Sergey Bravyi, Matthias Englbrecht, Robert König, and Nolan Peard. Correcting coherent errors with surface codes. *npj Quantum Information*, 4(1), October 2018.
- [38] Andrew S. Darmawan and David Poulin. Tensor-network simulations of the surface code under realistic noise. *Phys. Rev. Lett.*, 119:040502, Jul 2017.
- [39] Joel J. Wallman and Joseph Emerson. Noise tailoring for scalable quantum computation via randomized compiling. *Physical Review A*, 94(5), November 2016.
- [40] Nicolas Delfosse and Naomi H. Nickerson. Almost-linear time decoding algorithm for topological codes. *Quantum*, 5:595, December 2021.
- [41] Antonio deMarti iOlius, Patricio Fuentes, Román Orús, Pedro M. Crespo, and Josu Etxezarreta Martinez. Decoding algorithms for surface codes. *Quantum*, 8:1498, October 2024.
- [42] Hugo Perrin, Sven Jandura, and Guido Pupillo. Quantum error correction resilient against atom loss, 2024.
- [43] Hengyun Zhou, Chen Zhao, Madelyn Cain, Dolev Bluvstein, Casey Duckering, Hong-Ye Hu, Sheng-Tao Wang, Aleksander Kubica, and Mikhail D. Lukin. Algorithmic fault tolerance for fast quantum computing, 2024.
- [44] Kathleen Chang, Shraddha Singh, Jahan Claes, Kaavya Sahay, James Teoh, and Shruti Puri. Surface code with imperfect erasure checks, 2024.
- [45] In another word, this suggests that once a qubit is sampled to be leaked, we ignore subsequent instance suggesting its leakage again.
- [46] Anthony Ryan O’Rourke and Simon Devitt. Compare the pair: Rotated vs. unrotated surface codes at equal logical error rates, 2024.
- [47] Austin G. Fowler, Matteo Mariantoni, John M. Martinis, and Andrew N. Cleland. Surface codes: Towards practical large-scale quantum computation. *Phys. Rev. A*, 86:032324, Sep 2012.
- [48] Fern H E Watson and Sean D Barrett. Logical error rate scaling of the toric code. *New Journal of Physics*, 16(9):093045, September 2014.
- [49] Michael A. Nielsen and Isaac L. Chuang. *Quantum Computation and Quantum Information: 10th Anniversary Edition*. Cambridge University Press, 2010.
- [50] Yu Tomita and Krysta M. Svore. Low-distance surface codes under realistic quantum noise. *Physical Review A*, 90(6), December 2014.
- [51] Shouzhen Gu, Yotam Vaknin, Alex Retzker, and Aleksander Kubica. Optimizing quantum error correction protocols with erasure qubits, 2024.
- [52] Austin G Fowler and Kovid Goyal. Topological cluster state quantum computing. *arXiv preprint arXiv:0805.3202*, 2008.
- [53] Eric Dennis, Alexei Kitaev, Andrew Landahl, and John Preskill. Topological quantum memory. *Journal of Mathematical Physics*, 43(9):4452–4505, 2002.
- [54] Thomas M. Stace, Sean D. Barrett, and Andrew C. Doherty. Thresholds for topological codes in the presence of loss. *Phys. Rev. Lett.*, 102:200501, May 2009.
- [55] From the entropy of noise,  $\{Z_1 Z_2, I_1 I_2\}$  has lower entropy than  $\{Z_1, I_1\} \otimes \{Z_2, I_2\}$ . From decoding perspective, the former is easier to decode compared to the latter, with detector error model [32].
- [56] Oscar Higgott, Thomas C. Bohdanowicz, Aleksander Kubica, Steven T. Flammia, and Earl T. Campbell. Improved decoding of circuit noise and fragile boundaries of tailored surface codes, 2023.
- [57] Madelyn Cain, Chen Zhao, Hengyun Zhou, Nadine Meister, J. Pablo Bonilla Ataides, Arthur Jaffe, Dolev Bluvstein, and Mikhail D. Lukin. Correlated decoding of logical algorithms with transversal gates, 2024.
- [58] Nicolas Delfosse and Gilles Zémor. Linear-time maximum likelihood decoding of surface codes over the quantum

erasure channel. *Physical Review Research*, 2(3), July 2020.

### Appendix A: Gate operations and PTA in the presence of Leakage subspace

To study quantum operation in the presence of leaked state, we expand the qubit system ( $|0\rangle, |1\rangle$ ) to a qutrit system ( $|0\rangle, |1\rangle, |L\rangle$ ). The pauli matrix gives  $P'_i = P_i \oplus |L\rangle\langle L|$  ( $P_i = I, X, Y, Z$  is qubit pauli matrix). From hardware perspective, only state  $|11\rangle$  gains an additional phase  $e^{i\pi}$  so the gate operator gives  $CZ = I' \otimes I' - 2|11\rangle\langle 11|$ . For the jump operator  $K_1 = \sqrt{p_e}|L\rangle\langle 1|$ , it is easy to prove that it propagates a Z error using forward propagating as below

$$\begin{aligned} CZ I' \otimes K_1 CZ &= \sqrt{p_e}(I' \otimes I' - 2|11\rangle\langle 11|)(|0L\rangle\langle 01| + |1L\rangle\langle 11| + |LL\rangle\langle L1|)(I' \otimes I' - 2|11\rangle\langle 11|) \\ &= \sqrt{p_e}(|0L\rangle\langle 01| + |1L\rangle\langle 11| + |LL\rangle\langle L1|) \\ &= \sqrt{p_e}(|0\rangle\langle 0| - |1\rangle\langle 1| + |L\rangle\langle L|) \otimes |L\rangle\langle 1| = Z' \otimes K_1 \end{aligned} \quad (\text{A1})$$

The equation above naturally sets up for  $K_{1L}$ . For  $K_{0L}$ , we can prove that it do not propagate any error in the same way. Then we consider the condition that a leaked qubit interacts with three other unleaked qubit  $i, j, k$ . If the pauli matrix before this jump is X or Y, then the jump operator  $K_{0L}$  propagates to no error. Otherwise the jump operator  $K_{1L}$  propagates to  $Z_i Z_j Z_k$ . This error propagation is the core of our distance preserving property.

For the state (or density matrix) we consider, we assume that the density matrix can be written as the direct sum of qubit subspace and leakage subspace.

$$\rho = \rho_q \oplus \rho_L = \begin{bmatrix} \rho_{00} & \rho_{01} & 0 \\ \rho_{10} & \rho_{11} & 0 \\ 0 & 0 & \rho_{LL} \end{bmatrix} \quad (\text{A2})$$

With this equation, we can simply divide qubit subspace and leakage subspace when implementing PTA. This equation is also easy to satisfy from physical perspective because both BBR and RD are decoherence process [10].

Then we consider PTA in the presence of leaked state. The Kraus operator and channel of Rydberg decay is shown below (For clarity, we consider single qubit channel)

$$\begin{cases} K_0 = |0\rangle\langle 0| + \sqrt{1-p_e}|1\rangle\langle 1| + |L\rangle\langle L| \\ K_1 = \sqrt{p_e}|L\rangle\langle 1| \end{cases} \quad (\text{A3})$$

To implement PTA, we add an Pauli operator before and after that channel and average over the results, as below. Different from previous work, we use pauli matrix in the extend qutrit space.

$$\overline{\xi(\rho)^{P'}} = \frac{1}{4} \sum_{i=1}^4 P'_i \xi(P'_i \rho P'_i) P'_i = \frac{1}{4} \sum_{i=1}^4 P'_i \left( \sum_{j=0,1} K_j P'_i \rho P'_i K_j^\dagger \right) P'_i \quad (\text{A4})$$

We consider the no-jump evolution and jump operator separately by divide the sum over  $j$ . For no-jump evolution, the twirled channel gives  $(K_{0q} = |0\rangle\langle 0| + \sqrt{1-p_e}|1\rangle\langle 1| \approx (1 - \frac{p_e}{4})I + \frac{p_e}{4}Z)$

$$\begin{aligned} \overline{\xi_0(\rho)^{P'}} &= \frac{1}{4} \sum_{i=1}^4 P'_i (K_0 P'_i \rho P'_i K_0^\dagger) P'_i \\ &= \frac{1}{4} \sum_{i=1}^4 P_i \oplus |L\rangle\langle L| K_{0q} \oplus |L\rangle\langle L| P_i \oplus |L\rangle\langle L| \rho_q \oplus \rho_L P_i \oplus |L\rangle\langle L| K_{0q}^\dagger \oplus |L\rangle\langle L| P_i \oplus |L\rangle\langle L| \\ &= \left( \frac{1}{4} \sum_{i=1}^4 P_i K_{0q} P_i \rho_q P_i K_{0q}^\dagger P_i \right) \oplus \rho_L \\ &\approx \left[ \left(1 - \frac{p_e}{2} + \frac{p_e^2}{16}\right) I \rho_q I + \frac{p_e^2}{16} Z \rho_q Z \right] \oplus \rho_L \end{aligned} \quad (\text{A5})$$

The first term represents no-jump evolution in qubit subspace, which can be considered as Z error to second order of  $p_e$ . In our article, we take no account of this term. The second term represents that the state in leakage subspace

remains unchanged. The jump operator gives as below.

$$\begin{aligned}
\overline{\xi_1(\rho)}^{P'} &= \frac{1}{4} \sum_{i=1}^4 P'_i (K_1 P'_i \rho P'_i K_1^\dagger) P'_i \\
&= \frac{p_e}{4} \sum_{i=1}^4 P'_i |L\rangle \langle 1| P'_i \rho P'_i |1\rangle \langle L| P'_i \\
&= \frac{p_e}{4} \sum_{i=1}^4 |L\rangle \langle 1| P'_i \rho P'_i |1\rangle \langle L| \\
&= \frac{p_e}{4} |L\rangle \langle 1| \left[ \left( \sum_{i=1}^4 P_i \rho_q P_i \right) \oplus \rho_L \right] |1\rangle \langle L| \\
&= \frac{p_e}{2} (1 - \rho_{LL}) |L\rangle \langle L|
\end{aligned} \tag{A6}$$

The third equation comes from the fact that  $P'_i$  does not act on leaked state  $|L\rangle$ . And the final equation comes from  $\frac{I}{2} = \frac{\rho + X\rho X + Y\rho Y + Z\rho Z}{4}$  for an arbitrary density matrix in qubit subspace.  $(1 - \rho_{LL})$  is the trace of  $\rho_q$ . Eq.A6 show that with a random pauli matrix before jump operator just transform the biased-erasure channel to erasure channel. For this condition, we can not consider the error by adding random pauli error as usual in PTA. Instead, we start from the third line in Eq.A6. It can be considered as a part of the channel in operator-sum form ( $K_{0L} = \sqrt{\frac{p_e}{2}} |L\rangle \langle 0|$  and  $K_{1L} = \sqrt{\frac{p_e}{2}} |L\rangle \langle 1|$ ).

$$\begin{aligned}
\overline{\xi_1(\rho)}^{P'} &= \frac{p_e}{4} \sum_{i=1}^4 |L\rangle \langle 1| P'_i \rho P'_i |1\rangle \langle L| \\
&= K_{0L} \rho K_{0L}^\dagger + K_{1L} \rho K_{1L}^\dagger
\end{aligned} \tag{A7}$$

Therefore, if one qubit encounters a leakage during a CZ gate, the probability of  $K_{0L}$  and  $K_{1L}$  is 50% respectively. This can also be considered as sampling on the pauli matrix before the jump operator.  $X, Y$  corresponds to  $K_{0L}$  and  $I, Z$  corresponds to  $K_{1L}$ . We have studied the error propagation for the two jump operator  $K_{0L}$  and  $K_{1L}$ . After the jump operator is sampled, we study the error propagation as discussed above.

In our main text, we only consider CZ gates for the propose of generating RHG cluster state. The jump operators  $K_{0L}$  and  $K_{1L}$  do have deterministic error propagation for CZ gate but it is not a general condition for non-pauli error. For a jump operator  $K_{1L}$  in target qubit of CNOT gate  $CNOT = (I' \otimes I' - |11\rangle \langle 11| - |10\rangle \langle 10| + |10\rangle \langle 11| + |11\rangle \langle 10|)$ , the forward propagation gives

$$\begin{aligned}
CNOT I' \otimes K_{1L} CNOT &= \sqrt{p_e/2} CNOT(|0L\rangle \langle 01| + |1L\rangle \langle 11| + |LL\rangle \langle L1|) CNOT \\
&= \sqrt{p_e/2} (|0L\rangle \langle 01| + |1L\rangle \langle 10| + |LL\rangle \langle L1|) \\
&= \sqrt{p_e/2} (|0\rangle \langle 0| + |L\rangle \langle L|) \otimes |L\rangle \langle 1| + |1\rangle \langle 1| \otimes |L\rangle \langle 0| \\
&= \frac{1}{2} (I + Z') \otimes K_{1L} + \frac{1}{2} (I - Z') \otimes K_{0L}
\end{aligned} \tag{A8}$$

Namely, an error in a target of CNOT gate represented by  $K_{1L}$  will induce both  $K_{1L}$  and  $K_{0L}$ . This is a problem encountered when dealing with amplitude damping error error [34]. In our condition, we can utilize the freedom in operator-sum form of channel to define a set of kraus operator that is *structure preserving* in CNOT gate, as shown below ( $K_{+L} = \sqrt{\frac{p_e}{2}} |L\rangle \langle +|$  and  $K_{-L} = \sqrt{\frac{p_e}{2}} |L\rangle \langle -|$ ). It is easy to check that  $K_{-L}$  in target qubit propagates a  $Z$  error to control qubit while  $K_{+L}$  in target qubit does not propagate error. After these process, our protocol can be generalized to error correction codes with quantum circuit.

$$\begin{aligned}
\overline{\xi_1(\rho)}^{P'} &= \frac{p_e}{4} \sum_{i=1}^4 |L\rangle \langle 1| P'_i \rho P'_i |1\rangle \langle L| \\
&= K_{0L} \rho K_{0L}^\dagger + K_{1L} \rho K_{1L}^\dagger \\
&= K_{+L} \rho K_{+L}^\dagger + K_{-L} \rho K_{-L}^\dagger
\end{aligned} \tag{A9}$$

## Appendix B: Gate Sequence in the generation of RHG cluster state

The gate sequence in the generation of RHG cluster state needs discussion. Here, we select a clockwise gate sequence as is shown in Fig S1. This kind of gate sequence can separate proximal qubits when implementing CZ gate to different correlation surface. It can also be considered as an exchange between step 2 and step 3 of the initial proposed sequence (Fig.8 in [23]) and can be further simplified to two layers of atoms ([24] or Fig.14 in [23]).

Odd ( $2k+1$ ) layer of qubits

Even ( $2k+2$ ) layer of qubits

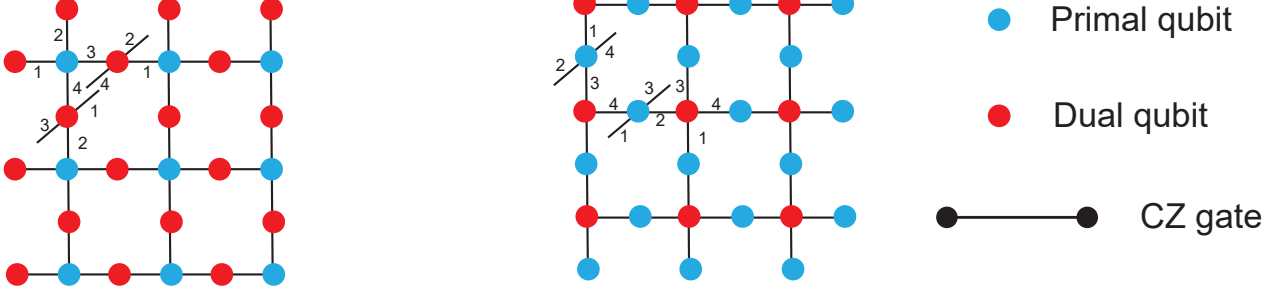


FIG. S1: Gate sequence of RHG cluster state

Now we prove that this gate sequence has separate all correlated error at the same correlation surface. We consider primal qubit as example and check whether one leakage error in dual qubit introduce correlated error at the same correlation surface. Since  $X_{dual}Z_1Z_2Z_3Z_4$  is a stabilizer of RHG cluster state and only  $Z$  operator flips the syndrome, we directly eliminate the error with pauli weight larger than 2. The result is shown in Table S1, no error chain introduce two-qubit error at the same correlation surface so it preserves full error distance.

Leakage instance \ Kraus operator	$L_1$	$L_2$	$L_3$	$L_4$
	$K_{0L}$	$I   Z_1$	$I   Z_2$	$I   Z_3$
$K_{1L}$	$Z_1   I$	$Z_3Z_4   Z_1$	$Z_4   Z_3Z_4$	$I   Z_4$

TABLE S1: Propagated error in 4 proximal qubits. The error before the vertical line represents  $L \otimes I$  instance otherwise  $L \otimes Z$  instance.  $Z_3Z_4$  is arranged in different correlation surface as shown in Fig S1.

## Appendix C: Erasure-like error in detector error model

In this appendix we discuss the erasure-like error and how to decode them in detector error model. See Fig.S2, if one dual qubit is measured to be leaked, it has four possible error sites. For each error site it introduce one or two error mechanisms. For  $L_1$ , the dephasing error equals to the propagated error up to a stabilizer and for  $L_4$  it does not propagate error. So these two only triggers single error mechanism.

We roughly divide the decoding in detector error model into two stages. First we need to sample the errors in CZ gates and then we need to add the error mechanisms to detector error model and convert it to a decoding graph in pymatching. For this step, all edges corresponding to the generate error has  $weight = 0$  and  $error\_probability = 0.5$ , which represents erasure channel. Second, we need to add edges by considering all possible error mechanisms (For one dual qubit, we need to consider 5 error mechanism as shown in Fig. S2), by changing their  $weight$  and leaving their  $error\_probability$  unchanged. After that, we have the decoding graph for erasure-like error and use pymatching to decode it.

The essence of erasure-like error lies in the fact that, the inferred probability is  $O(1)$  instead of  $O(p)$ . For example, if one dual qubit is leaked, we infer the forth primal qubit has  $1/4$  probability to have  $Z$  error. Therefore, when physical error rate  $p$  is small enough, erasure-like propagated  $Z$  errors have significant lower weight ( $w = \log \frac{1-p}{p}$ ) compared to conditional pauli error. The low weight edges help us locate the errors when we utilize MWPM algorithm to find matching with minimum weight, just like erasure error whose weight is 0 [49]. Our result in subsection V shows that

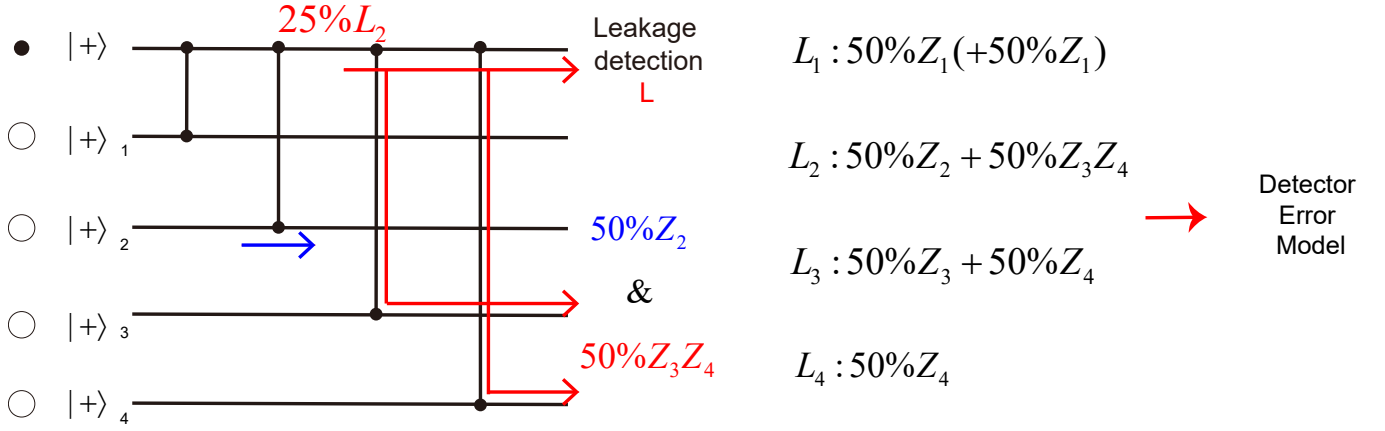


FIG. S2: Consider propagated error in detector error model. There are 4 possible error site if one dual qubit is measured to be leaked. Introduced error mechanism is listed and  $L_2$  is plotted for example. Once a Rydberg decay happens during CZ gate, it dephases the interacted primal qubit ( $50\%Z_2$ ) and propagates to Z error to remaining qubits ( $50\%Z_3Z_4$ ). For  $L_1$ , it dephases primal qubit 1 ( $50\%Z_1$ ) and propagates to  $50\%Z_2Z_3Z_4$  so it triggers two same error mechanism so we only account them once in detector error model.

a mixture of erasure error and *erasure-like* error still achieves error distance  $d_e = d$ . Some results in other works also verify the proof. However, we assume that *erasure-like* error can not perform better than erasure error. Because *erasure-like* errors only approximately locate the errors surrounding one leaked qubit, do not exactly tell the decoder which qubit is disturbed as erasure error. Another reason is that erasure error has smallest weight  $w = 0$ . (An edge with negative weight in decoding graph can be converted to positive weight by flipping the qubit so we assume  $w = 0$  is the smallest weight.) This insight is also related to our simplification of error model, as illustrated below. We consider one primal qubit with surrounding dual qubits and assume leakage happens in the first gate. Leakage (primal) - leakage (dual) and Leakage (primal) - tailored Z (dual) have exactly the same error in dual qubit because leakage error or erasure in the first primal qubit flips X basis measurement with 50% probability just as tailored Z error. But that qubit is erasure error located by physical detection instead of erasure-like error. Therefore,  $L \otimes L$  instance in CZ gates is a better case and we have considered the worse case  $L \otimes I$  and  $L \otimes Z$ .

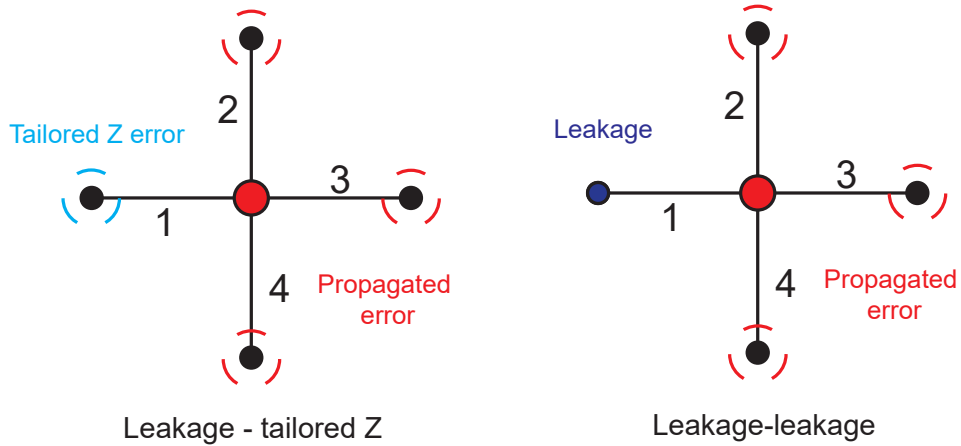


FIG. S3: Comparison between leakage-tailored Z instance and leakage-leakage instance: We consider one of these instance happens during the first CZ gates. The two instances have the same error in dual qubit. But the first dual qubit is *erasure-like* error by approximately located with proximal leaked primal qubit for leakage-tailored Z instance but is erasure error by physically detected for leakage-leakage instance.

### Appendix D: Several details in a more general error model

In this appendix we elaborate two details in our article to consider a more general error model. Total error rate  $p = p_e + p_p$  and  $R_e = \frac{p_e}{p}$ . To consider pauli error during CZ gates, we consider two-qubit depolarization error model. Namely we draw an operator from  $\frac{p_p}{15} \{I, X, Y, Z\}^{\otimes 2} \setminus \{I \otimes I\}$  for each CZ gate. We approximate depolarization error to first order. This approximation guarantees the accuracy of our decoding when  $p_p$  is small.

In RHG cluster state, primal lattice and dual lattice is decoded separately. For primal lattice, the stabilizers are the products of X operator of face qubits so only Z errors flip the stabilizers. X error in dual qubits propagate to several Z errors in primal qubits. Therefore, we only need to consider three types of error in two-qubit depolarization error model, namely  $\{Z_p, Y_p\} \otimes \{I_d, Z_d\}$ ,  $\{I_p, X_p\} \otimes \{X_d, Y_d\}$  and  $\{Z_p, Y_p\} \otimes \{X_d, Y_d\}$ , each type with probability  $\frac{4p_p}{15}$ .

First type is easy to consider, it can be considered as a single qubit pauli Z error with probability  $\frac{4p_p}{15}$  after each CZ gate. For the second type of error, X error in dual qubit after each CZ gate propagates to  $\{Z_1, Z_3, Z_4, I\}$ . For the first term, it suggests that a single qubit pauli X error with probability  $\frac{4p_p}{15}$  after the first CZ gate flips the primal qubit that implements the first CZ gate. We use the same method to consider the third type. Two-qubit depolarization error accounts for  $\frac{32p_p}{15}$  single qubit Z error for each primal qubit and  $\frac{8p_p}{15}$  hook error ( $Z_3Z_4$ ) for adjacent primal qubits in the third and fourth time sequence, to first order.

Consideration of biased erasure error is easy because the error model of CZ gate  $\{I, Z\}^{\otimes 2}$  commutes with CZ gates so we don't need to consider the error propagation. Therefore, for each CZ gate, there is  $p_e$  probability that the primal qubit encounters biased erasure. Final erasure probability is  $1 - (1 - p_e)^4$ . Depolarization error is considered in the same way with our method.

### Appendix E: Logical error rate comparison in small $p$ and large $d$ limit

In this appendix, we give extend discussion about sub-threshold scaling shown in Fig.6. In Fig.6, we show that the error distance of our method (LT) is slightly larger than that of erasure conversion. We are also interested in the performance when physical error rate is small enough and distance is large enough, since it is the general method to improve the accuracy of error correction.

When  $p$  is small enough, the logical error rate is governed by the error with shortest error chain. For a code with odd distance  $d$ ,  $d_e = \frac{d+1}{2}$  pauli errors trigger a logical error. When erasure error (erasure-like error) is in presence, one erasure or erasure-like error together with  $\frac{d-1}{2}$  pauli error is enough to introduce a logical error. So we write the logical error rate for LT and EC as the equations below (here,  $p = p_e + p_p$  and  $R_e$  is absorbed in  $c_p(d)$ ,  $c_{1e}(d)$  and  $c_{1el}(d)$ ).

$$\begin{cases} p_{L,EC} = c_p(d)p^{\frac{d+1}{2}} + c_{1e}(d)p^{\frac{d+1}{2}} + o(p^{\frac{d+1}{2}}) \\ p_{L,LT} = c_p(d)p^{\frac{d+1}{2}} + c_{1e}(d)p^{\frac{d+1}{2}} + c_{1el}(d)p^{\frac{d+1}{2}} + o(p^{\frac{d+1}{2}}) \end{cases} \quad (E1)$$

The ratio of logical error rate is  $\eta = 1 + \frac{c_{1el}(d)}{c_p(d) + c_{1e}(d)}$  we then prove two things: 1.  $\frac{c_{1el}(d)}{c_p(d)} \sim O(1)$  2.  $\frac{c_{1e}(d)}{c_p(d)} \sim O(d)$ .

*Proof:* To introduce a logical error, we need to sum over all possible shortest logical error chain whose length is  $\frac{d+1}{2}$ . For each selected error chain, it contributes to logical failure rate  $\sim (1 - R_e)^{\frac{d+1}{2}} p^{\frac{d+1}{2}}$  for pure pauli error. But for error chain with one erasure or erasure-like error, we first need to select a location to have erasure or erasure-like error, which has  $\frac{d+1}{2}$  situations. For error chain with one erasure error, it contributes to logical failure rate  $\sim \frac{d+1}{2} (1 - R_e)^{\frac{d-1}{2}} R_e p^{\frac{d+1}{2}}$ . For erasure-like error, the erasure-like error is likely to happen if one of the proximal dual qubits is leaked. So it contributes to logical failure rate  $\sim C \frac{d+1}{2} (1 - R_e)^{\frac{d-1}{2}} R_e p^{\frac{d+1}{2}}$ .  $C$  is determined by proximal qubits and the probability that a leaked dual qubit propagates to erasure-like error in primal lattice. We have above argument for each selected error chain so the conclusion preserves when summing over all possible error chains.

Given the discussion above, the ratio of logical error rate increases when  $d$  increases, but it converges to a constant for large  $d$ .

### Appendix F: Discussion and comparison with non-interacting loss model

In this appendix, we give some discussion about the error model used in two recent works [29, 42]. We refer to such model as non-interacting loss model, because they assume that the loss error does not dephase the interacted qubit. We emphasize that both their error model and our error model are proper [16]. Our error model includes both atom loss converted from BBR error and decay error. In fact, only decay error dephase the interacted qubit because we can assume all BBR error is converted to atom loss after the gate, so the Rydberg interaction remains unchanged during the gate. However, since our work deals with both errors uniformly, we need to account for the worst condition [16]. For the two works considering atom loss, non-interacting loss model is enough because they don't claim that they can deal with decay error. Our error model has better practical meaning because you can't only consider atom loss in experiment.

We also test the performance of our decoding protocol in non-interacting loss model. We assume that for each CZ gate one of the interacted qubit is lost with  $\frac{p_e}{2}$ . The results is shown in Fig. S4 and our decoding method also shows a high threshold 4.515% (It still has some space to improve since we don't optimize our reweighting till now). Our threshold is slightly lower than [29], which is a normal effect because we have used a matching based decoder while [29] uses a most-likely error (MLE) decoder. MLE decoder is the most accurate decoder but finding the most-likely error itself is a NP-hard problem and it is difficult to extend the decoder to large scale even with approximate MLE [29, 57]. However, different from the results in [57], MLE threshold for non-interacting loss model is only 2% larger than our matching-based decoder (about twice the threshold with MWPM in Table S1 in [57]). It is slightly counter-intuitive that a decoder with polynomial complexity [31] achieves a threshold very close to MLE, but we argue that it is reasonable because erasure channel has linear time but maximum likelihood decoding [58]. More works related to complexity of decoding algorithm of such erasure-like error is needed in the future.

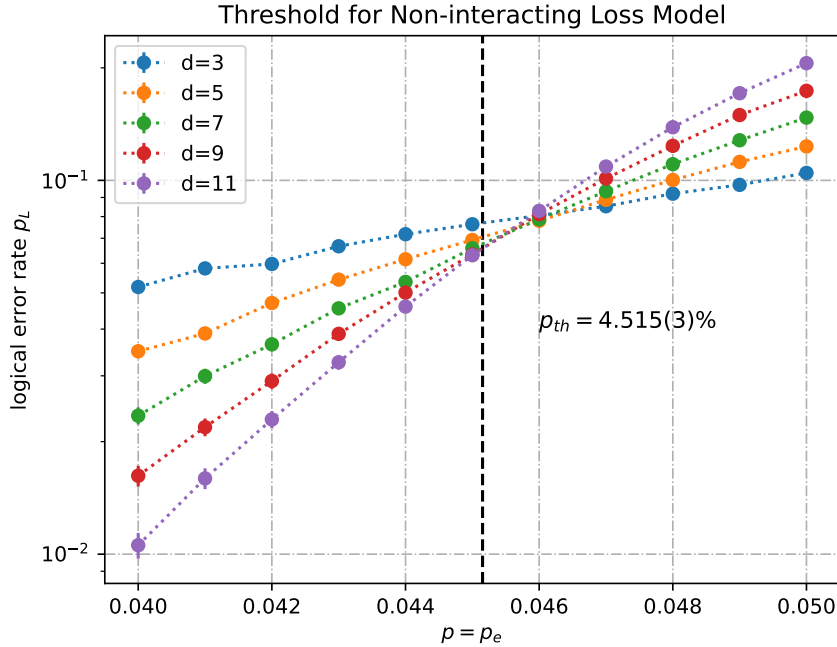


FIG. S4: Threshold for Non-interacting loss model: the threshold is derived from cross point of  $d = 9$  and  $d = 11$  and  $p_{th} = 4.515(3)\%$ .